

Improved Measurement of ttZ Couplings at the LHC

U. Baur^{*,1}, A. Juste^{†,2} and L.H. Orr[‡] and D. Rainwater^{§3}

¹*Dept. of Physics, State University of New York, Buffalo, NY 14260, USA*

²*Fermi National Accelerator Laboratory, Batavia, IL 60510, USA*

³*Dept. of Physics and Astronomy,
University of Rochester, Rochester, NY 14627, USA*

(Dated: November 2, 2018)

Abstract

We consider QCD $t\bar{t}Z$ production at the LHC with $Z \rightarrow \bar{\nu}\nu$ and all-hadronic $t\bar{t}$ decays, *i.e.* $pp \rightarrow \cancel{p}_T b\bar{b} + 4$ jets, as a tool to measure ttZ couplings. This channel has a significantly larger cross section than those where the Z boson decays leptonically. However, $t\bar{t}$, $b\bar{b} + 4$ jet, $t\bar{t}j$ and $t\bar{t}jj$ production give rise to potentially large backgrounds. We show that these processes can be suppressed to an acceptable level with suitable cuts, and find that adding the $\cancel{p}_T b\bar{b} + 4$ jet channel to the final states used in previous ttZ couplings analyses will improve the sensitivity by 10 – 60%. We also discuss how the measurement of the ttZ couplings may constrain Little Higgs models.

* baur@ubhex.physics.buffalo.edu

† juste@fnal.gov

‡ orr@pas.rochester.edu

§ rain@pas.rochester.edu

I. INTRODUCTION

Although the top quark was discovered more than ten years ago [1, 2], many of its properties are still only poorly known [3]. In particular, the couplings of the top quark to the electroweak (EW) gauge bosons have not yet been directly measured.¹ The large top quark mass [5] suggests that it may play a special role in EW symmetry breaking (EWSB). New physics connected with EWSB may thus be found first in top quark precision observables. A possible signal for new physics is a deviation of the any of the $tt\gamma$, ttZ or tbW couplings from the values predicted by the Standard Model (SM). For example, in technicolor and other models with a strongly coupled Higgs sector [6], and in Little Higgs models [7], anomalous top quark couplings may be induced at the 5 – 10% level.

Current data provide only weak constraints on the top quark couplings to EW gauge bosons, except for the ttZ vector and axial vector couplings, which are rather tightly but indirectly constrained by LEP/SLC Z -pole data (see Ref. [8] and references therein); and the right-handed tbW coupling, which is severely bounded by the observed $b \rightarrow s\gamma$ rate [9]. Future collider experiments offer many possibilities to probe the EW top quark couplings. The most promising ones with respect to the ttV ($V = \gamma, Z$) couplings are provided by an e^+e^- linear collider via $e^+e^- \rightarrow \gamma^*/Z^* \rightarrow t\bar{t}$ [10, 11, 12, 13, 14, 15, 16], and the LHC via $t\bar{t}V$ production [8, 17, 18].

At an e^+e^- linear collider operating at $\sqrt{s} = 500$ GeV and with an integrated luminosity of $100 - 200 \text{ fb}^{-1}$, one could measure the ttV couplings in top pair production with a few-percent precision [13]. However, the process $e^+e^- \rightarrow \gamma^*/Z^* \rightarrow t\bar{t}$ is sensitive to both $tt\gamma$ and ttZ couplings simultaneously, and significant cancellations between the various couplings can occur. At hadron colliders, $t\bar{t}$ production is so dominated by the QCD processes $gg, q\bar{q} \rightarrow t\bar{t}$ that a measurement of the EW neutral couplings via $q\bar{q} \rightarrow \gamma^*/Z^* \rightarrow t\bar{t}$ is hopeless. Instead, they can be measured in QCD $t\bar{t}Z/\gamma$ production and radiative top quark decays in $t\bar{t}$ events ($t\bar{t} \rightarrow \gamma W^+W^- b\bar{b}$). Each of the processes is sensitive to the EW couplings of only the boson emitted: Z and photon independently. This obviates having to disentangle potential cancellations between the different couplings. In these three processes one can also hope to separate the dimension-four and -five couplings which appear in the effective Lagrangian describing ttV interactions.

In Ref. [8] we presented a detailed analysis of $t\bar{t}V$ production at hadron colliders. We found that while the $tt\gamma$ couplings can be measured at the LHC with a precision of typically a few percent, the bounds on the ttZ couplings are a factor 3 – 10 weaker, in particular for the vector and axial vector couplings, F_{1V}^Z and F_{1A}^Z . A major factor which limits their sensitivity is the relatively small cross section for $t\bar{t}Z$ production when one requires the Z boson to decay leptonically (where we mean $\ell^+\ell^-$ ($\ell = e, \mu$) throughout), as in our previous analysis.

In this paper, we extend our $t\bar{t}Z$ analysis to the case where the $t\bar{t}$ pair decays hadronically and the Z boson decays into neutrinos. Due to the larger branching ratio for $Z \rightarrow \bar{\nu}\nu$ relative to leptonic decays, this effectively triples the number of events which can be utilized, thus our present analysis may significantly improve the limits on anomalous ttZ couplings. However, the increased statistics comes at the price of a background which is potentially much larger than the signal. After reviewing the definition of the ttZ couplings, we present

¹ Although the measurement of the W boson helicity in top quark decay [4] may be regarded as a constraint on top quark couplings.

a detailed discussion of the signal and all relevant backgrounds (Sec. II), showing that the most important backgrounds can be adequately suppressed by imposing suitable cuts. In Sec. III we derive sensitivity bounds for the $b\bar{b}\bar{\nu}\nu+4j$ final state and combine them with those we obtained previously [8]. We also explore how a ttZ coupling measurement at the LHC may help constrain parameters of Little Higgs models. We summarize our findings in Sec. IV.

II. CALCULATION OF SIGNAL AND BACKGROUND

A. Definition of general ttZ couplings

The most general Lorentz-invariant vertex function describing the interaction of a Z boson with two top quarks can be written in terms of ten form factors [19], which are functions of the kinematic invariants. In the low energy limit, these correspond to couplings which multiply dimension-four or -five operators in an effective Lagrangian, and may be complex. If the Z boson couples to effectively massless fermions, the number of independent form factors is reduced to eight. In addition, if both top quarks are on-shell, the number is further reduced to four. In this case, the ttZ vertex can be written in the form

$$\Gamma_{\mu}^{ttZ}(k^2, q, \bar{q}) = -ie \left\{ \gamma_{\mu} (F_{1V}^Z(k^2) + \gamma_5 F_{1A}^Z(k^2)) + \frac{\sigma_{\mu\nu}}{2m_t} (q + \bar{q})^{\nu} (iF_{2V}^Z(k^2) + \gamma_5 F_{2A}^Z(k^2)) \right\}, \quad (1)$$

where e is the proton charge, m_t is the top quark mass, q (\bar{q}) is the outgoing top (anti-top) quark four-momentum, and $k^2 = (q + \bar{q})^2$. The terms $F_{1V}^Z(0)$ and $F_{1A}^Z(0)$ in the low energy limit are the ttZ vector and axial vector form factors. The coefficients $F_{2V}^Z(M_Z^2)$ and $F_{2A}^Z(M_Z^2)$, where M_Z is the Z boson mass, are related to the the weak magnetic and (CP -violating) weak electric dipole moments, g_t^Z and d_t^Z . At tree level in the SM,

$$F_{1V}^{Z,SM} = -\frac{1}{4 \sin \theta_W \cos \theta_W} \left(1 - \frac{8}{3} \sin^2 \theta_W \right), \quad F_{1A}^{Z,SM} = \frac{1}{4 \sin \theta_W \cos \theta_W},$$

$$F_{2V}^{Z,SM} = 0, \quad F_{2A}^{Z,SM} = 0,$$

where θ_W is the weak mixing angle. The numerically most important radiative corrections to the vector and axial vector couplings can be taken into account by replacing the factor $(1 - 8 \sin^2 \theta_W/3)$ in $F_{1V}^{Z,SM}$ by $(1 - 8 \sin^2 \theta_{eff}^t/3)$, where $\sin^2 \theta_{eff}^t$ is the effective mixing angle; and by expressing the remaining factors of $\sin \theta_W$ and $\cos \theta_W$ in $F_{1V,A}^{Z,SM}$ in terms of the physical W and Z masses. Numerically, the one-loop corrections to $F_{1V,A}^Z$ are typically of $\mathcal{O}(10^{-2} - 10^{-3})$ [20]. The weak magnetic dipole form factor F_{2V}^Z receives contributions of the same magnitude [21] at the one-loop level in the SM. However, there is no such contribution to the weak electric dipole form factors, F_{2A}^Z [19].

S -matrix unitarity restricts $\Delta F_{1V,A}^Z(0) = F_{1V,A}^Z(0) - F_{1V,A}^{Z,SM}$ to be $\lesssim \mathcal{O}(1)$ if the scale of new physics is of the order of a few TeV [8, 22].

B. Signal

The process $pp \rightarrow t\bar{t}Z$ with leptonic Z boson decay was considered in detail in Ref. [8]. Here we concentrate on final states where $Z \rightarrow \bar{\nu}\nu$. Since the $t\bar{t}Z$ cross section is too small to

be observable at the Tevatron, we concentrate our efforts on the LHC. The neutrinos escape undetected and, thus, manifest themselves in the form of missing transverse momentum, \cancel{p}_T . If one or both W bosons originating from the top decay, $t \rightarrow Wb$, decay leptonically, the observed states, $\ell\cancel{p}_T b\bar{b}jj$ and $\ell\ell'\cancel{p}_T b\bar{b}$, are identical to those resulting from ordinary $t\bar{t}$ production. As the $t\bar{t}$ cross section is more than a factor 1000 larger than that of $t\bar{t}Z$, it will be very difficult to sufficiently suppress this background. We therefore consider only the case where both W bosons decay hadronically,

$$pp \rightarrow \cancel{p}_T b\bar{b} + 4j. \quad (2)$$

We assume that both b quarks are tagged with a combined efficiency of $\epsilon_b^2 = 0.4$. Note that, since there is essentially no phase space for $t \rightarrow WZb$ decays ($BR(t \rightarrow WZb) \approx 3 \cdot 10^{-6}$ [23, 24]), $t\bar{t}$ production with one top decaying into WZb does not contribute to the final state of Eq. (2).

We perform our calculation for general $t\bar{t}Z$ couplings of the form of Eq. (1). At LHC energies, Z boson transverse momenta of at most a few hundred GeV are accessible in $t\bar{t}Z$ production. The scale of new physics responsible for anomalous $t\bar{t}Z$ couplings would be expected to be of $\mathcal{O}(1 \text{ TeV})$ or higher. Form factor effects will thus be small and are therefore neglected in the following. We also assume that all $t\bar{t}Z$ couplings are real. We otherwise assume the SM to be valid. Our calculation includes top quark and Z boson decays with full spin correlations and finite width effects. All top quark resonant Feynman diagrams are included. To ensure gauge invariance of the SM result, we use the so-called overall-factor scheme of Ref. [25] as implemented in the MADGRAPH [26]-derived code of Ref. [27].

All signal and background cross sections in this paper are computed using CTEQ6L1 [28] parton distribution functions with the strong coupling constant evaluated at leading order and $\alpha_s(M_Z^2) = 0.130$. We set the top quark mass to $m_t = 178 \text{ GeV}$ [29].² All signal cross sections in this paper are calculated for factorization and renormalization scales equal to m_t .

The basic acceptance cuts for $\cancel{p}_T b\bar{b} + 4j$ events at the LHC are

$$\begin{aligned} p_T(b) > 20 \text{ GeV}, & \quad |\eta(b)| < 2.5, & \quad \Delta R(b, b) > 0.4, \\ p_T(j) > 30 \text{ GeV}, & \quad |\eta(j)| < 2.5, & \quad \Delta R(j, j) > 0.4, & \quad \Delta R(j, b) > 0.4, \end{aligned} \quad (3)$$

where $\Delta R = [(\Delta\phi)^2 + (\Delta\eta)^2]^{1/2}$ is the separation in pseudorapidity–azimuth space. We include minimal detector effects via Gaussian smearing of parton momenta according to CMS [31] expectations, and take into account the b jet energy loss via a parameterized function. To ensure that the LHC experiments can trigger on the events of interest, we require at least three (b - or non- b) jets to have

$$p_T(j) > 50 \text{ GeV} \quad (4)$$

and

$$\cancel{p}_T > 5 \text{ GeV}^{1/2} \sqrt{\sum p_T}, \quad (5)$$

where the sum extends over jets and b quarks in the final state. Furthermore, to reduce the background from non-resonant $Zb\bar{b} + 4j$ production and singly-resonant processes such as

² A recent update of the Tevatron top mass analysis using Run II data has resulted in a slightly lower value, $m_t = 172.7 \text{ GeV}$ [30]. This value leads to a marginally higher $t\bar{t}Z$ cross section.

$pp \rightarrow t\bar{t}Zjj$, we require that the two b quarks and four jets are consistent with originating from a $t\bar{t}$ pair. This is accomplished by selecting events which satisfy

$$\chi_{min}^2 = \min_{b_1j_1j_2b_2j_3j_4 \text{ perm}} [\chi^2(b_1j_1j_2; b_2j_3j_4)] < 3 \quad (6)$$

where χ_{min}^2 is the minimum of the $\chi^2(b_1j_1j_2; b_2j_3j_4)$ values of all possible combinations of jet pairs and bjj combinations, and

$$\chi^2(b_1j_1j_2; b_2j_3j_4) = \frac{(m(j_1j_2) - M_W)^2}{\sigma_W^2} + \frac{(m(j_3j_4) - M_W)^2}{\sigma_W^2} + \frac{(m(b_1j_1j_2) - m_t)^2}{\sigma_t^2} + \frac{(m(b_2j_3j_4) - m_t)^2}{\sigma_t^2}. \quad (7)$$

For the $W \rightarrow jj$ and $t \rightarrow bjj$ invariant mass resolutions we take $\sigma_W = 7.8$ GeV and $\sigma_t = 13.4$ GeV [32].

As we discuss in more detail below, potentially large backgrounds arise from ordinary $t\bar{t}$ and $b\bar{b}+4j$ production where the four momentum vector of one or more jets is badly mismeasured. In contrast to signal events, the azimuthal opening angle $\Delta\phi(\not{p}_T, p_T(b\bar{b}))$ between the missing transverse momentum and the transverse momentum of the two b quarks,

$$\mathbf{p}_T(b\bar{b}) = \mathbf{p}_T(b) + \mathbf{p}_T(\bar{b}) \quad (8)$$

in $t\bar{t}$ and $b\bar{b}+4j$ background events is typically smaller than 90° . The same is also true for the azimuthal opening angle $\Delta\phi(\not{p}_T, p_T(had))$ between the missing transverse momentum and the transverse momentum of the four leading non- b jets,

$$\mathbf{p}_T(had) = \sum_{i=1}^4 \mathbf{p}_T(j_i). \quad (9)$$

In addition to the cuts listed in Eqs. (3)–(6), we therefore require

$$\Delta\phi(\not{p}_T, p_T(b\bar{b})) > 100^\circ, \quad \Delta\phi(\not{p}_T, p_T(had)) > 100^\circ. \quad (10)$$

Imposing the cuts listed in Eqs. (3)–(10), and before taking into account b -tagging efficiencies, we obtain a signal cross section of about 3.4 fb.

C. Background processes

The potentially most dangerous irreducible background to $\not{p}_T b\bar{b}+4j$ production originates from $t\bar{t}j$ production, where one top quark decays hadronically, $t \rightarrow Wb \rightarrow bjj$, and the other via $t \rightarrow Wb \rightarrow \tau\nu_\tau b$ with the τ -lepton decaying hadronically, $\tau \rightarrow h\nu_\tau$. We calculate this process using tree level matrix elements which include all decay correlations. Because of its small mass and typically high transverse momentum, we simulate τ decays in the collinear approximation. All τ decays are calculated following the approach described in Ref. [33]. For the probability that a τ -jet is misidentified as a light quark/gluon jet we assume a constant value of $P_{h \rightarrow j} = 20\%$. Ref. [34] found that $P_{h \rightarrow j}$ decreases with increasing jet transverse momentum, from 20% for $p_T(j) = 20$ GeV to 5% at $p_T(j) = 60$ GeV. Our results for the $t\bar{t}j$ background thus should be regarded as conservative.

Other contributions to the irreducible background arise from singly-resonant top quark production ($t\bar{b}Zjj$ and $\bar{t}bZjj$), and from non-resonant $WZb\bar{b}jj$ and $Zb\bar{b} + 4j$ production. The calculation of these backgrounds was discussed in detail in Ref. [8] for $Z \rightarrow \ell^+\ell^-$ decays. It is straightforward to adapt the calculation to $Z \rightarrow \bar{\nu}\nu$ decays. Finally, $t\bar{t}jj$ production with $t\bar{t} \rightarrow \tau^+\nu_\tau\tau^-\bar{\nu}_\tau b\bar{b}$ and both τ -leptons decaying hadronically has to be considered. We calculate this background using ALPGEN [35], treating τ decays the same as for the $t\bar{t}j$ background discussed above.

There are also several reducible backgrounds which result from missing transverse momentum arising from badly-mismeasured jet momenta, or from not detecting a charged lepton. The main contributions to the first category arise from $t\bar{t}$, $b\bar{b}+4j$ and $6j$ production. We calculate the latter two processes using ALPGEN. QCD $6j$ production contributes only if two light jets are misidentified as b jets. To estimate the contribution of this process we assume the probability for a light jet to be misidentified as a b jet to be $P_{j \rightarrow b} = 1/100$. QCD $t\bar{t}jj$ production contributes to the background if $t\bar{t} \rightarrow \ell^\pm\nu_\ell b\bar{b}jj$ ($\ell = e, \mu$) and the charged lepton is missed. Likewise, $pp \rightarrow t\bar{t}W$ contributes if the $t\bar{t}$ system decays hadronically, $t\bar{t} \rightarrow b\bar{b}+4j$, and the lepton in $W \rightarrow \ell\nu$ is missed; or if $t\bar{t} \rightarrow \ell^\pm\nu_\ell b\bar{b}jj$ and $W \rightarrow jj$. We assume that an electron or muon is missed if $|\eta(\ell)| > 2.5$, $p_T(\ell) < 10$ GeV, or if either $\Delta R(\ell, j) < 0.4$ or $\Delta R(\ell, b) < 0.4$. Since electrons can be detected, albeit with reduced efficiency, at rapidities larger than 2.5 using the forward electromagnetic calorimeter, our estimates of the $t\bar{t}jj$ and $t\bar{t}W$ backgrounds are conservative. We calculate the $t\bar{t}jj$ background again using ALPGEN.

Our calculation of the $t\bar{t}j(j)$ backgrounds does not include contributions from $t\bar{t}(j)$ production where one or both top quarks decay radiatively, $t \rightarrow Wbj(j)$. Due to the \cancel{p}_T and χ^2 cuts of Eqs. (5) and (6), such contributions are strongly suppressed.

In Fig. 1 we show the missing transverse momentum distributions for the SM $t\bar{t}Z$ signal (solid curve) and for various backgrounds. The \cancel{p}_T requirement of Eq. (5) implies that $\cancel{p}_T > 80$ GeV. The most important backgrounds originate from $t\bar{t}jj$ and $t\bar{t}j$ production. However, the missing transverse momentum distribution from these processes falls considerably faster than that of the signal: for $\cancel{p}_T > 300$ GeV, the SM signal dominates. The $t\bar{t}W$ background (dotted line) is about one order of magnitude smaller than the signal. The $t\bar{t}$ (dashed line) and $b\bar{b}+4j$ (histogram) backgrounds are important only at low values of \cancel{p}_T . Since the missing transverse momentum in these events originates entirely from b -decays and mismeasurements, their \cancel{p}_T distributions fall very rapidly. This is even more the case for the $6j$ background which we found to essentially vanish after cuts. The $t\bar{t}jj$, $t\bar{t} \rightarrow \tau^+\nu_\tau\tau^-\bar{\nu}_\tau b\bar{b} \rightarrow \cancel{p}_T b\bar{b}jj$ background is found to be about four orders of magnitude smaller than the signal, thus is not shown.

The background contributions of $Zb\bar{b}+4j$, calculated with ALPGEN [35], and $WZb\bar{b}jj$, $t\bar{b}Zjj$ and $\bar{t}bZjj$ production, calculated with MADEVENT [36], are not shown in Fig. 1. As discussed in Ref. [8], these cross sections are one to two orders of magnitude smaller than the signal and can safely be neglected here.

It should be noted that the background cross sections as calculated at tree level depend significantly on the choice of factorization and renormalization scales, μ_F and μ_R , which were taken to be $\mu_F = \mu_R = m_t$ in all cases, even for backgrounds without resonant top quarks. Including next-to-leading order (NLO) corrections in most cases significantly reduces the scale dependence of a process. Unfortunately, the NLO QCD corrections are not presently known for any of the background processes, except for $t\bar{t}$ production [32, 37]. However, as we shall discuss in Sec. III A, it may be possible to extract the background cross sections using data. For the dominant $t\bar{t}j(j)j$ backgrounds this should provide a more accurate estimate

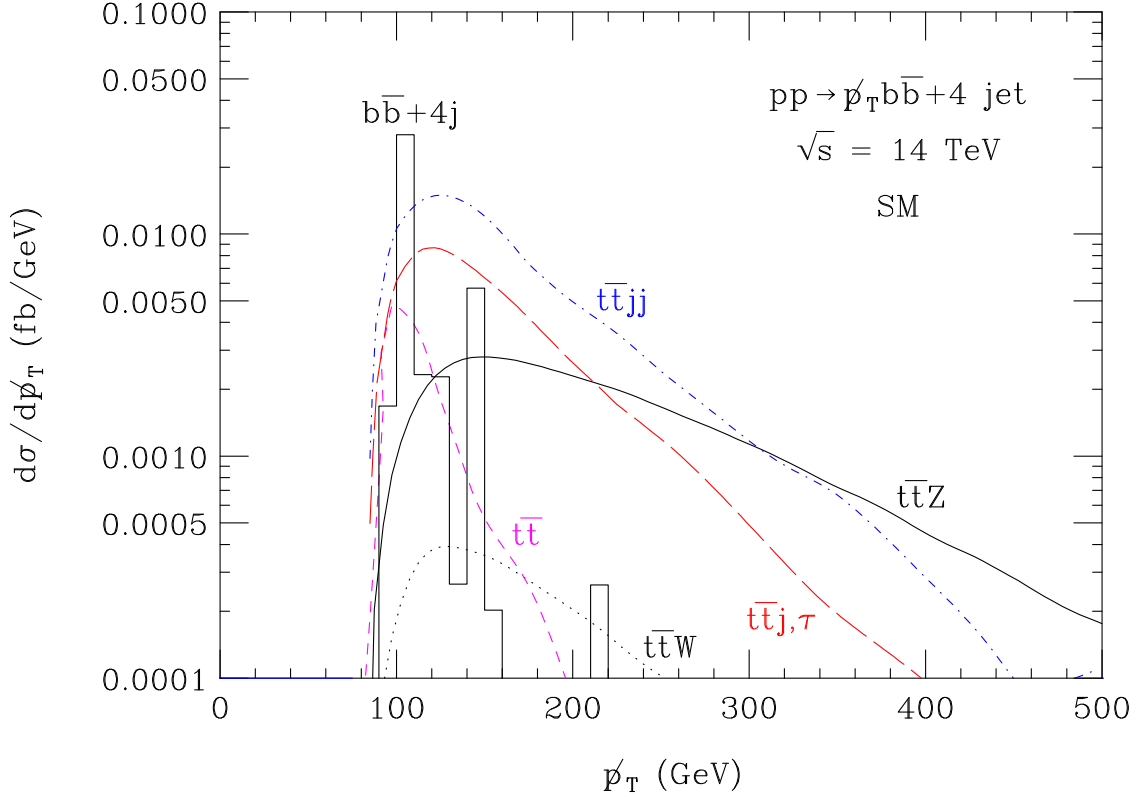


Figure 1: The differential cross sections as a function of missing transverse momentum for $p_T b\bar{b} + 4j$ production at the LHC. Shown are the SM predictions for $t\bar{t}Z$ production and various backgrounds. We impose the cuts of Eqs. (3–10), but do not include the double b -tag efficiency common to all curves.

of the cross section than the leading order QCD predictions.

The p_T distribution for $pp \rightarrow t\bar{t}Z$ in the SM (after decays), and for various anomalous ttZ couplings, together with the combined p_T distribution of the $t\bar{t}$, $b\bar{b} + 4j$, $t\bar{t}j$ and $t\bar{t}jj$ backgrounds, are shown in Fig. 2. Only one coupling at a time is allowed to deviate from its SM prediction. Fig. 2 shows that, as in the case when the Z boson decays leptonically [8], varying $F_{1V,A}^Z$ leads mostly to a normalization change of the SM signal cross section, hardly affecting the shape of the p_T distribution. Thus, the low- p_T region contributes most of the statistical weight when extracting bounds on $F_{1V,A}^Z$. Since the signal p_T distribution is approximately proportional to $(F_{1V}^Z)^2 + (F_{1A}^Z)^2$, it is difficult to disentangle vector and axial vector couplings in the $p_T b\bar{b} + 4j$ final state.³ Furthermore, $F_{1V,A}^Z = F_{1V,A}^{Z,SM}$ and $F_{1V,A}^Z = -F_{1V,A}^{Z,SM}$ yield approximately the same cross sections.

The dimension five couplings, $F_{2V,A}^Z$, on the other hand, lead to a missing transverse momentum distribution significantly harder than that predicted by the SM. As a result, most of the sensitivity to $F_{2V,A}^Z$ originates from the high- p_T region. While the background is about one order of magnitude larger than the signal close to p_T threshold, it is smaller than the signal for $p_T > 380$ GeV. As a result, the limits extracted for $F_{2V,A}^Z$ depend considerably

³ In $t\bar{t}Z$ final states with $Z \rightarrow \ell^+ \ell^-$, other distributions, such as the azimuthal (transverse plane) opening angle between the charged leptons, may be used to help discriminate between F_{1V}^Z and F_{1A}^Z [8].

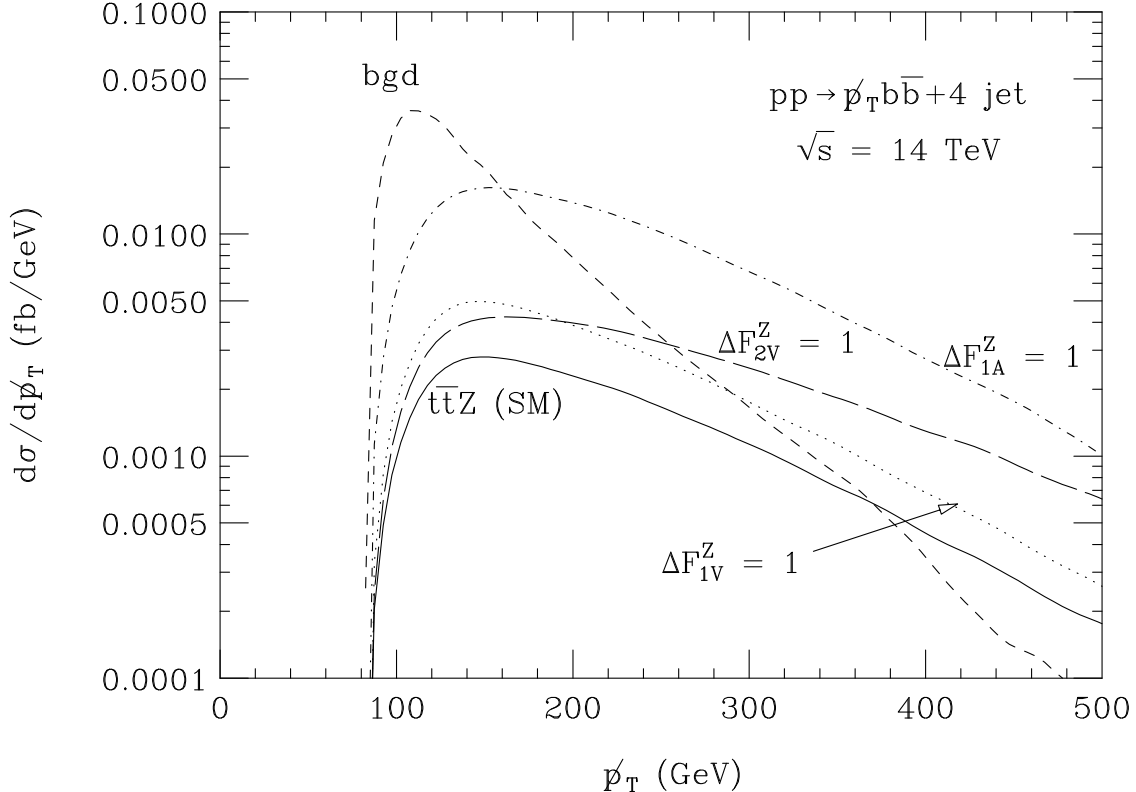


Figure 2: The differential cross sections as a function of missing transverse momentum for $p_T b \bar{b} + 4j$ production at the LHC. Shown are the SM predictions for $t\bar{t}Z$ production (solid line), the combined $t\bar{t}$, $b\bar{b} + 4j$, $t\bar{t}j$ and $t\bar{t}jj$ background, and the predictions for several non-standard ttZ couplings. Only one coupling at a time is allowed to deviate from its SM value. We impose the cuts of Eqs. (3–10), but do not include the double b -tag efficiency common to all curves.

less on the background than those for $F_{1V,A}^Z$.

As stated before, we require that both b quarks be tagged. A looser requirement of at least one tagged b quark would result in a signal cross section increase of a factor $(2/\epsilon_b - 1)$, about 2.2 using our b -tagging assumption. But this larger signal rate comes at the expense of an increased background. In particular, the $6j$ and $b\bar{b} + 4j$ backgrounds increase drastically due to the larger combinatorial background from grouping jets and the tagged b quark. Detailed calculations would be needed for a quantitative estimate of the increase. However, since the single- b -tagged background is probably considerably larger than that for the double b -tagged channel, we do not consider it here.

III. ANOMALOUS COUPLINGS LIMITS AND MODEL IMPLICATIONS

A. Limits on anomalous ttZ couplings

The shape and normalization changes of the p_T spectrum can be used to derive quantitative sensitivity bounds on anomalous ttZ couplings. We do this by performing a log-likelihood test on the distribution and calculating 68% confidence level (CL) limits. To calculate the statistical significance, we split the p_T distribution into bins, each with typi-

cally more than five events. We impose the cuts described in Sec. IIB and assume a double b -tag efficiency of $\epsilon_b^2 = 0.4$. Except for the ttZ couplings we assume the SM to be valid: the tbW and ttg couplings can be independently and precisely measured at the LHC in single top [38] and $t\bar{t}$ production [32], respectively. We perform multi-parameter fits for the different anomalous couplings, which we assume to be real.

The log-likelihood function we use to compute confidence levels is

$$-2 \log L = -2 \left[\sum_i (-f_S S_i - f_B B_i + n_{0i} \log(f_S S_i + f_B B_i) - \log(n_{0i}!)) \right] + \frac{(f_S - 1)^2}{(\Delta f_S)^2} + \frac{(f_B - 1)^2}{(\Delta f_B)^2}, \quad (11)$$

where the sum extends over the number of bins, S_i and B_i are the number of signal and background events in the i th bin, and n_{0i} is the number of SM events in the i th bin. The uncertainties on the signal and background normalizations are taken into account via two multiplicative factors, f_S and f_B , which are allowed to vary but are constrained within the relative uncertainties of the signal and background cross sections, Δf_S and Δf_B , respectively.

To derive sensitivity bounds, we take into account the dominant $t\bar{t}jj$, $t\bar{t}j$, $t\bar{t}$ and $b\bar{b}+4j$ backgrounds. We calculate limits for 300 fb^{-1} and 3000 fb^{-1} . An integrated luminosity of 300 fb^{-1} corresponds to 3 years of running at the LHC design luminosity of $\mathcal{L} = 10^{34} \text{ cm}^{-2} \text{ s}^{-1}$, while the larger value of 3000 fb^{-1} can be achieved in about 3 years of running at the luminosity-upgraded LHC (SLHC) [39].

As mentioned in Sec. II, the dimension five couplings $F_{2V,A}^Z$ lead to a considerably harder \not{p}_T distribution than that predicted by the SM. Most of the sensitivity to these couplings thus originates from the high missing transverse momentum region. In this region, the signal to background ratio is of $\mathcal{O}(1)$ or better (cf. Fig. 2). The sensitivity bounds on $F_{2V,A}^Z$ should therefore depend very little on the normalization uncertainties of signal and background.

For $F_{1V,A}^Z$, however, the situation is different. Since the vector and axial vector couplings essentially change only the overall normalization of the $t\bar{t}Z$ cross section, precise knowledge of the SM signal cross section is very important. Most of the sensitivity to $F_{1V,A}^Z$ comes from the region of small \not{p}_T where the background dominates over the signal. The achievable bounds on these couplings are thus expected to depend sensitively on the signal and background cross section uncertainties.

As explained before, except for the $t\bar{t}$ background, QCD corrections for neither the signal nor the background cross sections are known. The cross sections of the main backgrounds, $t\bar{t}jj$ and $b\bar{b}+4j$ production, are proportional to α_s^4 and α_s^6 , respectively, whereas the signal cross section scales as α_s^2 . The background thus depends more strongly on the factorization and renormalization scales than the signal. Its normalization can be fixed by relaxing the selection cuts (Eqs. (6) and (10)), measuring the cross section in a background-dominated region of phase space, and then extrapolating to the analysis region. Since the cross sections for $t\bar{t}jj$ and $b\bar{b}+4j$ production are large, this should make it possible to determine the background with an uncertainty (Δf_B) of a few percent, provided that the systematic uncertainties can be adequately controlled and that the QCD corrections do not significantly change the shape of the \not{p}_T distribution of the background. Exactly how well this will work in practice remains an open question.

To reduce the signal cross section uncertainty, the NLO QCD corrections to $t\bar{t}Z$ production must be calculated. This appears to be feasible with current techniques. Once the corrections are known, the remaining uncertainty (Δf_S) is likely to be of order 10%.

To derive quantitative sensitivity limits for anomalous ttZ couplings, we assume $\Delta f_S = 0.1$ and $\Delta f_B = 0.05$. Unfortunately, the minimization of $-2 \log L$ with respect to f_S and f_B cannot be performed analytically. Doing it numerically becomes very time consuming when more than one of the ttZ couplings are varied at the same time. However, if one does not allow the signal and background normalizations to vary independently, *i.e.* if $f_S = f_B = f$, $\log L$ can be minimized analytically. In this case, one finds the minimum of $\log L$ to occur at

$$f = \frac{1}{2} \left(1 - (\Delta f)^2 N + \sqrt{(1 - (\Delta f)^2 N)^2 + 4(\Delta f)^2 N_0} \right), \quad (12)$$

where

$$N = \sum_i (S_i + B_i) \quad (13)$$

is the total number of events,

$$N_0 = \sum_i n_{0i} \quad (14)$$

the total number of SM events, and Δf is the SM cross section uncertainty. The computer time required to derive sensitivity limits for anomalous ttZ couplings is now much reduced.

The 68% CL bounds on $\Delta F_{1V,A}^Z$ we obtain for $\Delta f_S = 0.1$ and $\Delta f_B = 0.05$ agree with those derived for $f_S = f_B = f$ and $\Delta f = 0.3$ within 10 – 30%. In view of the current signal and background cross section uncertainties, an analysis with $f_S = f_B = f$ and $\Delta f = 0.3$ when all couplings are varied should be sufficient. At first, it may be somewhat surprising that one needs Δf to be significantly larger than Δf_S and Δf_B in order to arrive at similar bounds for non-standard ttZ couplings. However, varying the signal and background cross section normalizations separately allows for changes in both the normalization and the shape of the SM cross section. On the other hand, requiring $f_S = f_B = f$ allows for only a change in the normalization. Since the anomalous ttZ coupling sensitivity results from both normalization and \not{p}_T distribution shape changes, taking into account the uncertainty on both naturally has a relatively larger impact than if only the normalization uncertainty is included in the analysis. One can partially compensate for this effect by increasing Δf .

Our results are shown in Figs. 3 and 4, and in Table I. Fig. 3 shows the correlations between various anomalous ttZ couplings for an integrated luminosity of 300 fb^{-1} ; Fig. 4 displays the bounds one can hope to achieve at the SLHC with 3000 fb^{-1} . Shown are the results for the $\not{p}_T b\bar{b} + 4j$ final state (dashed lines), the combined limits from the dilepton and trilepton final states analyzed in Ref. [8] (dotted lines), and the limits resulting from combining all final states (solid lines). Including the $\not{p}_T b\bar{b} + 4j$ final state in the extraction of bounds improves the limits by 10 – 60%. For an integrated luminosity of 300 fb^{-1} , it will be possible to measure the ttZ axial vector coupling with a precision of about 10%, and $F_{2V,A}^Z$ with a precision of 40%. At the SLHC, these bounds can be improved by factors of about 1.6 ($F_{2V,A}^Z$) and 2.3 – 3 (F_{1A}^Z). The achievable bounds on F_{1V}^Z are much weaker than those projected for F_{1A}^Z : as mentioned in Sec. III, the \not{p}_T distributions for the SM and for $F_{1V,A}^Z = -F_{1V,A}^{Z,SM}$ are almost degenerate. As a result, an area centered at $\Delta F_{1V,A}^Z = -2F_{1V,A}^{Z,SM}$ remains, which cannot be excluded, even at the SLHC where one expects several thousand $t\bar{t}Z$ events. For F_{1V}^Z , the two regions merge, resulting in rather poor limits. For F_{1A}^Z , the two regions are distinct. Since the area centered at $\Delta F_{1A}^Z = -2F_{1A}^{Z,SM}$ is incompatible with the indirect limits on the ttZ vector and axial vector couplings from Z -pole data [8], we do not include this area in Table I or Figs. 3 and 4.

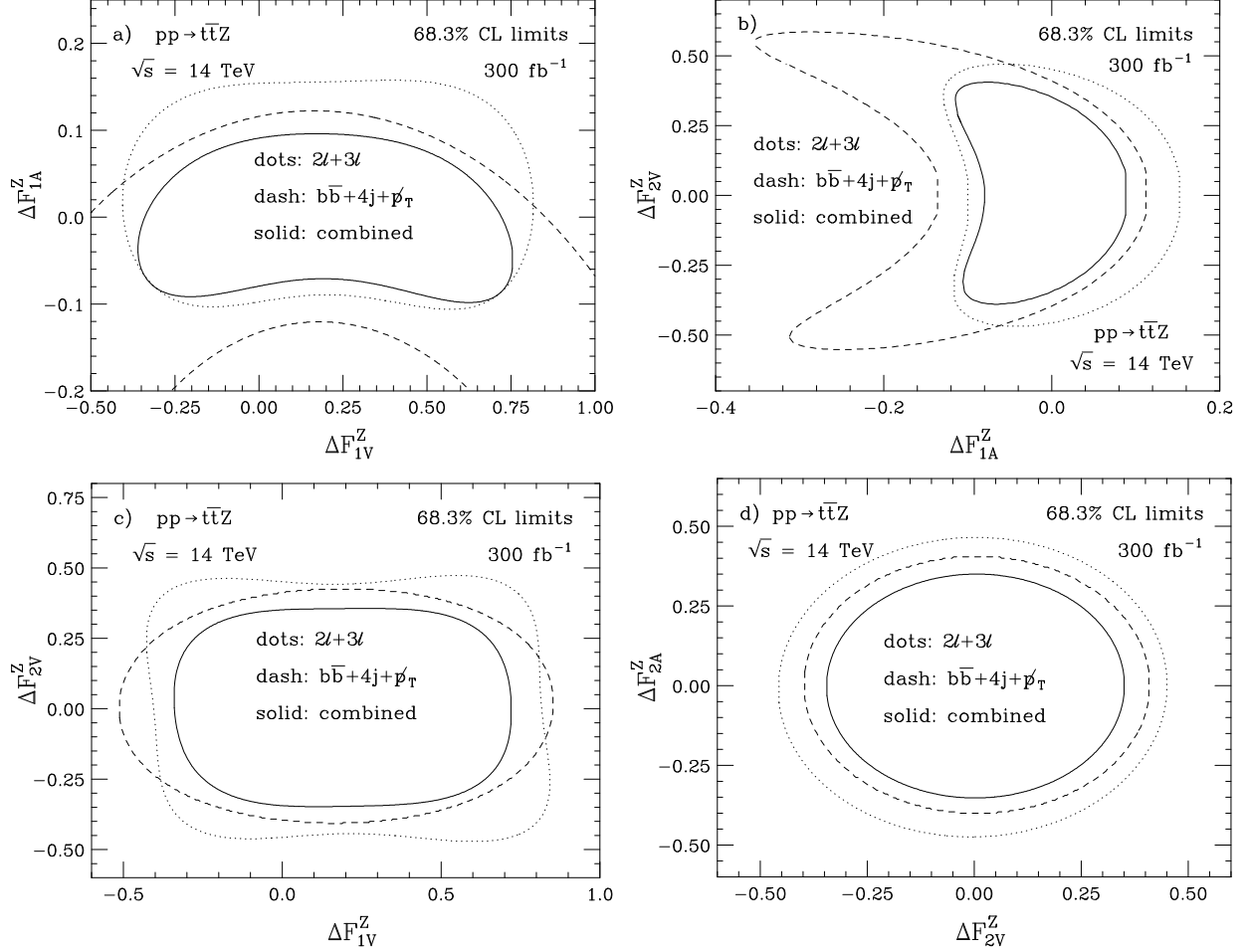


Figure 3: Projected 68.3% CL bounds on anomalous ttZ couplings from the LHC with an integrated luminosity of 300 fb^{-1} , for: (a) ΔF_{1A}^Z versus ΔF_{1V}^Z , (b) ΔF_{2V}^Z versus ΔF_{1A}^Z , (c) ΔF_{2V}^Z versus ΔF_{1V}^Z , and (d) ΔF_{2A}^Z versus ΔF_{2V}^Z . Shown are the limits obtained from the $p_T b\bar{b}+4j$ (dashed) and the dilepton and trilepton final states (dotted), and the combined limits (solid). To derive limits for the dilepton and trilepton final states, we use the results of Ref. [8]. In each graph, only those couplings which are plotted against each other are assumed to be different from their SM values.

While the bounds on ΔF_{1A}^Z improve by 20–60% when the $p_T b\bar{b}+4j$ channel is included in the analysis, the gain is limited to about 10% for ΔF_{1V}^Z . The global limits on the dimension-five couplings $F_{2V,A}^Z$ improve by about 20%. However, if only F_{2V}^Z and F_{2A}^Z are varied, including the $p_T b\bar{b}+4j$ final state strengthens their bounds by about 35%. The relatively larger importance of the $p_T b\bar{b}+4j$ channel in this case can be understood by recalling that most of the sensitivity to the dimension-five couplings originates from high p_T values where the background is less important. This allows one to take better advantage of the larger $p_T b\bar{b}+4j$ final state cross section.

The correlations between F_{2A}^Z and F_{1A}^Z (F_{2A}^Z and F_{1V}^Z) are similar to those for F_{2V}^Z and F_{1A}^Z (F_{2V}^Z and F_{1V}^Z), thus are not shown in Figs. 3 and 4.

The ttZ couplings are indirectly constrained by precision Z -pole data collected at LEP and SLC. Vector and axial vector couplings are bound by Z -boson data to within a few percent of their SM values if one assumes that no other sources of new physics contribute.

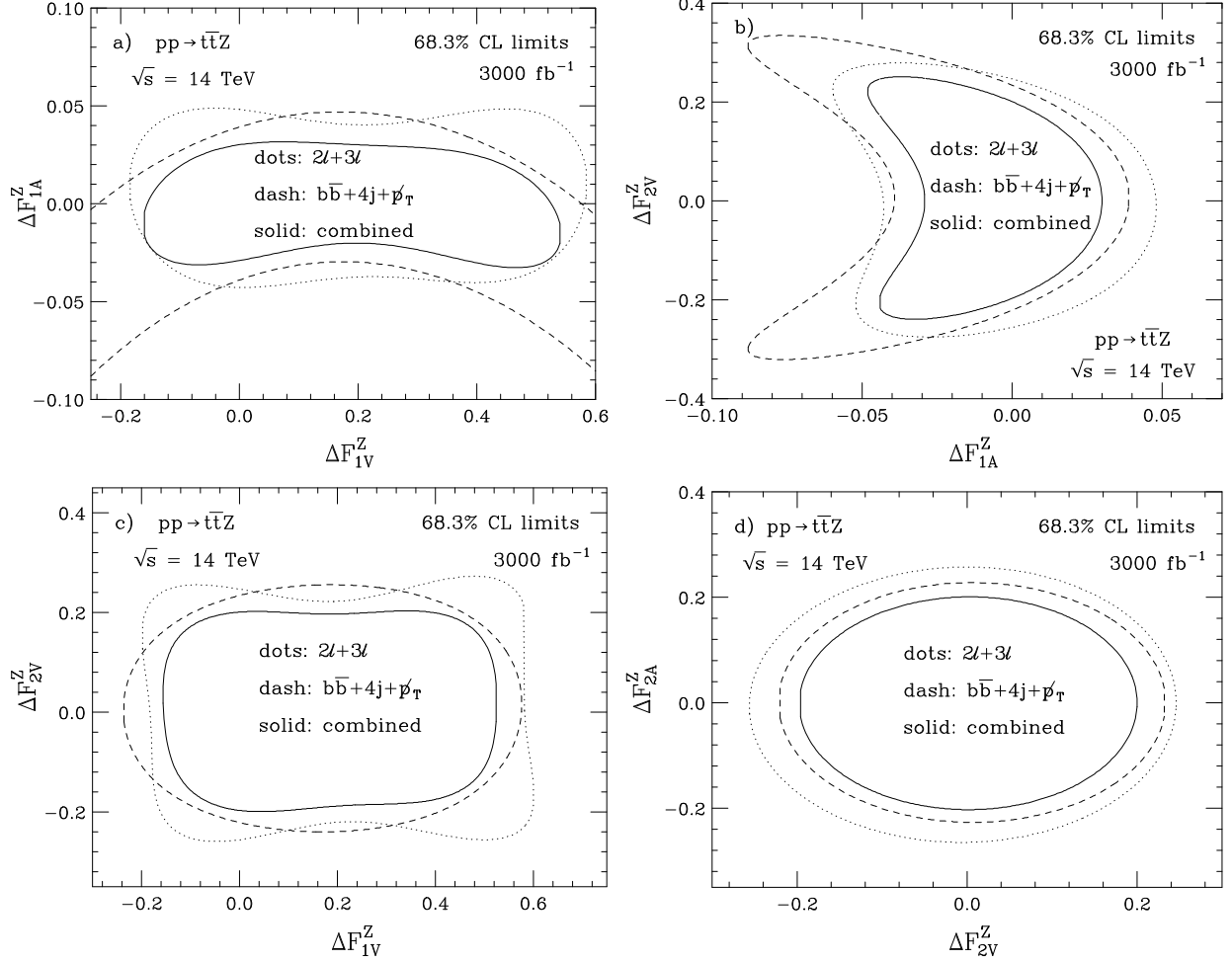


Figure 4: Projected 68.3% CL bounds on anomalous ttZ couplings from the SLHC with an integrated luminosity of 3000 fb^{-1} , for: (a) ΔF_{1A}^Z versus ΔF_{1V}^Z , (b) ΔF_{2V}^Z versus ΔF_{1A}^Z , (c) ΔF_{2V}^Z versus ΔF_{1V}^Z , and (d) ΔF_{2A}^Z versus ΔF_{2V}^Z . Shown are the limits obtained from the $p_T b\bar{b}+4j$ (dashed) and the dilepton and trilepton final states (dotted), and the combined limits (solid). To derive limits for the dilepton and trilepton final states, we use the results of Ref. [8]. In each graph, only those couplings which are plotted against each other are assumed to be different from their SM values.

In contrast, the limits obtained for F_{2V}^Z are much weaker, $|F_{2V}^Z| \lesssim \mathcal{O}(0.2)$, and depend on the value of the anomalous magnetic moment of the top quark [40]. The effect of F_{2A}^Z on LEP/SLC observables has not yet been studied. Thus, $t\bar{t}Z$ production at the LHC will provide valuable information on the dimension-five couplings. Since the LEP/SLC constraints arise from one-loop corrections which diverge for non-standard ttZ couplings, they are cutoff-dependent. When taking into account the $p_T b\bar{b}+4j$ final state, the achievable sensitivity on F_{1A}^Z at the SLHC begins to approach that of the indirect bounds from Z -pole data. For the ttZ vector coupling, it will be impossible to match that precision at the LHC, even for an integrated luminosity of 3000 fb^{-1} and including the $p_T b\bar{b}+4j$ final state in the analysis.

The ttZ couplings can also be tested in $e^+e^- \rightarrow t\bar{t}$. However, as mentioned in Sec. I, the process $e^+e^- \rightarrow \gamma^*, Z^* \rightarrow t\bar{t}$ is sensitive to both $tt\gamma$ and ttZ couplings simultaneously. If only one coupling at a time is allowed to deviate from its SM value, a linear e^+e^- collider operating

300 fb ⁻¹ (LHC)				3000 fb ⁻¹ (SLHC)			
coupling	$\not{p}_T b\bar{b}+4j$	$2\ell+3\ell$	combined	coupling	$\not{p}_T b\bar{b}+4j$	$2\ell+3\ell$	combined
ΔF_{1V}^Z	–	+0.84 –0.43	+0.75 –0.36	ΔF_{1V}^Z	–	+0.60 –0.18	+0.54 –0.16
ΔF_{1A}^Z	+0.12 –	+0.16 –0.13	+0.096 –0.112	ΔF_{1A}^Z	+0.047 –	+0.049 –0.060	+0.031 –0.048
ΔF_{2V}^Z	+0.59 –0.55	+0.47 –0.47	+0.38 –0.39	ΔF_{2V}^Z	+0.34 –0.32	+0.28 –0.28	+0.25 –0.24
ΔF_{2A}^Z	+0.57 –0.58	+0.48 –0.49	+0.40 –0.40	ΔF_{2A}^Z	+0.33 –0.33	+0.28 –0.29	+0.25 –0.25

Table I: Sensitivities achievable at 68.3% CL for anomalous ttZ couplings at the LHC and SLHC for integrated luminosities of 300 fb⁻¹, and 3000 fb⁻¹. The limits shown represent the maximum and minimum values obtained when taking into account the correlations between any possible pair of anomalous couplings. Results are for the $\not{p}_T b\bar{b}+4j$ final state, the combined dilepton and trilepton final states analyzed in Ref. [8] (labeled $2\ell+3\ell$), and for all channels combined. The cuts imposed are described in Sec. II B.

at $\sqrt{s} = 500$ GeV with an integrated luminosity of 100 – 200 fb⁻¹ would be able to probe *all* ttZ couplings with a precision of 1 – 5% [13]. With the possible exception of F_{1A}^Z , a linear collider will thus be able to significantly improve the sensitivity limits expected from the LHC, even when the $\not{p}_T b\bar{b}+4j$ channel is included and assuming 3000 fb⁻¹ from the SLHC. It should be noted, however, that this picture could change once cancellations between different non-standard ttZ couplings, and between $tt\gamma$ and ttZ couplings, are allowed. While beam polarization at an e^+e^- collider would provide a very powerful tool to disentangle the effects of different couplings, unfortunately no realistic studies on the simultaneous measurement of couplings in $e^+e^- \rightarrow t\bar{t}$ have been performed so far.

B. Constraints on Little Higgs parameter space

As noted in Sec. I, the ttZ couplings may deviate substantially from their SM values in Little Higgs (LH) models. Here we explore how their measurement at the LHC may constrain parameter space in the $SU(5)/SO(5)$ Littlest Higgs model with T-parity [41, 42, 43]. In this model, the ttZ vector and axial vector couplings are modified by mixing of the left-handed top quark and a heavy top quark partner, T . One finds

$$\Delta F_{1V}^Z = -\Delta F_{1A}^Z = \frac{\lambda_T^2 v^2}{2m_T^2} F_{1A}^{Z,SM}, \quad (15)$$

where λ_T is the tTh coupling (h is the Higgs boson), $v \approx 246$ GeV is the SM Higgs vacuum expectation value, and m_T is the T quark mass. Eq. (15) and the log likelihood function can be used to derive lower 68.3% CL limits for m_T/λ_T :

$$\frac{m_T}{\lambda_T} \geq 600 \text{ GeV} \quad \text{for } 300 \text{ fb}^{-1}, \quad (16)$$

$$\frac{m_T}{\lambda_T} \geq 1000 \text{ GeV} \quad \text{for } 3000 \text{ fb}^{-1}. \quad (17)$$

For comparison, current EW precision data require $m_T/\lambda_T > 650$ GeV [44]. We thus expect the SLHC will be able to improve this bound, while the LHC should be able to discover a T

quark with a mass of $m_T \leq 2$ TeV with 300 fb^{-1} of data [45]. If a T -quark candidate were found, a measurement of F_{1A}^Z would be valuable in helping to pin down λ_T .

In LH models without T-parity, anomalous ttZ couplings may receive additional contributions from mixing of the W and Z bosons with a heavy $SU(2)$ triplet of vector bosons, W_H^\pm and W_H^3 , which are characteristic for LH models [7]. However, constraints from precision EW data severely restrict these additional contributions.

IV. SUMMARY AND CONCLUSIONS

Currently, little is known about top quark couplings to the Z boson. There are no direct measurements of these couplings; indirect measurements, using LEP and SLC data, tightly constrain only the ttZ vector and axial vector couplings. The ttZ couplings could be measured directly in $e^+e^- \rightarrow t\bar{t}$ at a future e^+e^- linear collider. However, such a machine is at least a decade away. In addition, the process $e^+e^- \rightarrow t\bar{t}$ is simultaneously sensitive to $tt\gamma$ and ttZ couplings, and significant cancellations between various couplings may occur.

In this paper, we considered $t\bar{t}Z$ production with $Z \rightarrow \bar{\nu}\nu$ and $t\bar{t} \rightarrow b\bar{b}+4j$ at the LHC as a tool to measure ttZ couplings. At the Tevatron, the $t\bar{t}Z$ cross section is too small to be observable. When the Z boson decays leptonically, the small $Z \rightarrow \ell^+\ell^-$ branching ratio is one of the main factors which limits the achievable sensitivity to anomalous ttZ couplings. The larger $Z \rightarrow \bar{\nu}\nu$ branching ratio (relative to $Z \rightarrow \ell^+\ell^-$) effectively triples the number of signal events and thus has the potential to significantly improve the sensitivity to non-standard couplings.

We calculated the signal cross sections taking into account all top quark-resonant Feynman diagrams. All relevant background processes were included in estimating limits on the couplings. Once $t\bar{t}Z$ selection cuts are imposed, the background drops significantly faster with missing transverse momentum than the signal, and for $p_T > 380$ GeV the signal dominates. The largest background source is $t\bar{t}jj$ production, where one of the top quarks decays semi-leptonically and the charged lepton is lost. In all our calculations we assumed that both b quarks are tagged, to bring the backgrounds to a controllable level.

Our analysis reveals that the achievable sensitivity limits utilizing final states where the Z decays leptonically [8] can be improved by 10 – 60% when the $p_T b\bar{b}+4j$ mode is taken into account. The improvement is particularly pronounced for the ttZ axial vector coupling F_{1A}^Z which can be measured with a precision of 3 – 5% at the luminosity-upgraded LHC (3000 fb^{-1}). Measuring F_{1A}^Z with such precision will make it possible constrain the parameter space in Little Higgs models which predict deviations of the ttZ vector and axial vector couplings of up to 10%.

Acknowledgments

We would like to thank J. Parsons, G. Watts and J. Womersley for useful discussions. One of us (U.B.) would like to thank the Fermilab Theory Group, where part of this work was carried out, for its generous hospitality. This research was supported in part by the National Science Foundation under grant No. PHY-0139953 and the Department of Energy under grant DE-FG02-91ER40685. Fermilab is operated by Universities Research Association Inc.

under Contract No. DE-AC02-76CH03000 with the U.S. Department of Energy.

- [1] F. Abe *et al.* (CDF Collaboration), Phys. Rev. Lett. **74**, 2626 (1995).
- [2] S. Abachi *et al.* (DØ Collaboration), Phys. Rev. Lett. **74**, 2632 (1995).
- [3] D. Chakraborty, J. Konigsberg and D. Rainwater, Ann. Rev. Nucl. Part. Sci. **53**, 301 (2003).
- [4] D. Acosta *et al.* (CDF collaboration), Phys. Rev. **D71**, 031101 (2005) [Erratum-ibid. **D71**, 059901 (2005)];
V. M. Abazov *et al.*, (DØ Collaboration), Phys. Lett. **B617**, 1 (2005);
V. M. Abazov *et al.* (DØ Collaboration), Phys. Rev. **D72**, 011104(R) (2005);
V. M. Abazov *et al.* (DØ Collaboration), Phys. Rev. **D72**, 011104 (2005).
- [5] S. Eidelman *et al.*, Phys. Lett. **B592**, 1 (2004), and 2005 partial update for the 2006 edition available at the PDG WWW page (URL: <http://pdg.lbl.gov>).
- [6] R. S. Chivukula, S. B. Selipsky and E. H. Simmons, Phys. Rev. Lett. **69**, 575 (1992);
R. S. Chivukula, E. H. Simmons and J. Terning, Phys. Lett. **B331**, 383 (1994);
K. Hagiwara and N. Kitazawa, Phys. Rev. **D52**, 5374 (1995);
U. Mahanta, Phys. Rev. **D55**, 5848 (1997) and Phys. Rev. **D56**, 402 (1997).
- [7] C. F. Berger, M. Perelstein and F. Petriello, arXiv:hep-ph/0512053.
- [8] U. Baur, A. Juste, L. H. Orr and D. Rainwater, Phys. Rev. **D71**, 054013 (2005).
- [9] F. Larios, M. A. Perez and C. P. Yuan, Phys. Lett. **B457**, 334 (1999);
M. Frigeni and R. Rattazzi, Phys. Lett. **B269**, 412 (1991).
- [10] B. Grzadkowski and Z. Hioki, Phys. Rev. **D61**, 014013 (2000).
- [11] B. Grzadkowski and Z. Hioki, Nucl. Phys. **B585**, 3 (2000).
- [12] Z. H. Lin *et al.*, Phys. Rev. **D65**, 014008 (2002).
- [13] T. Abe *et al.* (American Linear Collider Working Group Collaboration), in *Proc. of the APS/DPF/DPB Summer Study on the Future of Particle Physics (Snowmass 2001)* ed. N. Graf, arXiv:hep-ex/0106057.
- [14] J. A. Aguilar-Saavedra *et al.* (ECFA/DESY LC Phys. Working Group) arXiv:hep-ph/0106315.
- [15] R. Frey, arXiv:hep-ph/9606201.
- [16] G. A. Ladinsky and C. P. Yuan, Phys. Rev. **D49**, 4415 (1994).
- [17] H. Y. Zhou, arXiv:hep-ph/9806323.
- [18] U. Baur, M. Buice and L. H. Orr, Phys. Rev. **D64**, 094019 (2001).
- [19] W. Hollik *et al.*, Nucl. Phys. **B551**, 3 (1999) [Erratum-ibid. **B557**, 407 (1999)].
- [20] W. F. L. Hollik, Fortsch. Phys. **38**, 165 (1990).
- [21] J. Bernabeu, D. Comelli, L. Lavoura and J. P. Silva, Phys. Rev. **D53**, 5222 (1996).
- [22] M. Hosch, K. Whisnant and B. L. Young, Phys. Rev. **D55**, 3137 (1997).
- [23] G. Mahlon and S. J. Parke, Phys. Lett. **B347**, 394 (1995).
- [24] G. Altarelli, L. Conti and V. Lubicz, Phys. Lett. **B502**, 125 (2001);
R. Decker, M. Nowakowski and A. Pilaftsis, Z. Phys. **C57**, 339 (1993);
E. Jenkins, Phys. Rev. **D56**, 458 (1997).
- [25] U. Baur, J. A. M. Vermaseren and D. Zeppenfeld, Nucl. Phys. **B375**, 3 (1992).
- [26] T. Stelzer, F. Long, Comput. Phys. Commun. **81** (1994) 357.
- [27] F. Maltoni, D. L. Rainwater and S. Willenbrock, Phys. Rev. **D66**, 034022 (2002).
- [28] J. Pumplin *et al.*, JHEP **0207**, 012 (2002).
- [29] V. M. Abazov *et al.* (DØ Collaboration), Nature **429**, 638 (2004), and references therein.

- [30] J. F. Arguin *et al.* (the Tevatron Electroweak Working group), arXiv:hep-ex/0507091.
- [31] M. Della Negra *et al.* (CMS Collaboration), CMS Letter of Intent, CERN-LHCC-92-3;
G. L. Bayatian *et al.* (CMS Collaboration), CMS Tech. Design Report, CERN-LHCC-94-38.
- [32] M. Beneke *et al.*, arXiv:hep-ph/0003033 and references therein.
- [33] D. Rainwater, D. Zeppenfeld and K. Hagiwara, Phys. Rev. **D59**, 014037 (1999);
T. Plehn, D. Rainwater and D. Zeppenfeld, Phys. Lett. **B454**, 297 (1999)
and Phys. Rev. **D61**, 093005 (2000).
- [34] D. Cavalli and S. Resconi, ATLAS physics note 98-118 (January 1998).
- [35] M. L. Mangano *et al.*, JHEP **0307**, 001 (2003).
- [36] F. Maltoni and T. Stelzer, JHEP **0302**, 027 (2003).
- [37] M. L. Mangano, P. Nason and G. Ridolfi, Nucl. Phys. **B373**, 295 (1992);
S. Frixione, M. L. Mangano, P. Nason and G. Ridolfi, Phys. Lett. **B351**, 555 (1995).
- [38] E. Boos, L. Dudko and T. Ohl, Eur. Phys. J. **C11**, 473 (1999).
- [39] F. Gianotti *et al.*, Eur. Phys. J. **C39**, 293 (2005).
- [40] O. J. P. Eboli, M. C. Gonzalez-Garcia and S. F. Novaes, Phys. Lett. **B415**, 75 (1997).
- [41] H. C. Cheng and I. Low, JHEP **0309**, 051 (2003).
- [42] H. C. Cheng and I. Low, JHEP **0408**, 061 (2004).
- [43] I. Low, JHEP **0410**, 067 (2004).
- [44] J. Hubisz, P. Meade, A. Noble and M. Perelstein, arXiv:hep-ph/0506042.
- [45] G. Azuelos *et al.*, Eur. Phys. J. **C39S2**, 13 (2005).